NANO LETTERS

2009
Vol. 9, No. 5
1994-1998

Mesoporous ZnS Nanorattles: Programmed Size Selected Access to Encapsulated Enzymes

Dara Van Gough,[†,‡,§] Alejandro Wolosiuk,[⊥,#] and Paul V. Braun*[,†,‡,§]

Department of Materials Science and Engineering, Beckman Institute, and Frederick Seitz Materials Research Laboratory, University of Illinois at Urbana−Champaign, Urbana, Illinois 61801, Gerencia Química, CNEA, CAC Av. Gral Paz 1499, B1650KNA, Buenos Aires, Argentina, and DQIAyQF, FCEN, Universidad de Buenos Aires, Ciudad Universitaria, Pabellón II, C1428EHA, Buenos Aires, Argentina

Received January 25, 2009; Revised Manuscript Received March 14, 2009

ABSTRACT

A size selective nanorattle was formed by encapsulating soybean peroxidase (SBP) within a ZnS mesoporous hollow sphere. Once encapsulated within the mesoporous hollow sphere, the SBP remained active against molecules smaller than the 3 nm diameter of the mesopores in the shell wall, while molecules larger than the mesopores, which could not pass into the hollow sphere, did not interact with the SBP. Specifically, encapsulated SBP catalyzed the oxidation of Amplex Ultra-Red, a small fluorogen, in the presence of hydrogen peroxide, encapsulated SBP was deactivated by sodium azide, and no reaction was observed between encapsulated SBP and a greater than 3 nm diameter protease.

Viruses are recognized as being highly developed responsive nanocontainers and delivery vehicles. The cowpea chlorotic mottle virus (CCMV) capsid, for example, contains chemically responsive pores, which controllably release a payload when triggered.[1] The selective permeability of the CCMV viral capsid has been utilized to package both inorganic and organic species, including iron oxide,[2] paratungstate,[3] and poly(anetholsulfonic acid).[3] A number of approaches to synthetically mimic these fascinating structures have been investigated. For example, with colloidal particles as a starting point, hollow organic,[4] inorganic,[5,6] or composite[7] nanocontainers, including some which are responsive to environmental stimuli, e.g., pH,[8,9] ionic strength,[9] and temperature,[10] can be produced.

Chemically functionalized mesoporous materials represent another interesting class of materials that mimic the chemical responsivity of viral capsids.[11,12] Mesoporous systems have attracted considerable interest for a variety of potential applications,[13] in part because their characteristic pore size can be defined over a size range similar to many important biological macromolecules, and the pores can be chemically functionalized to modify their properties. For example, nanovalves, formed by binding cyclobis(paraquat-*p*-phenylene) to [2]pseudorotaxanes attached to mesoporous silica, have been used to control the release of an entrapped organometallic complex.[14] One flexible route to synthesize mesoporous materials, lyotropic liquid crystal templating, is often used due to its simplicity, degree of control over the structure of the product materials, and applicability to a broad range of materials, including metals,[15] oxides,[16] and chalcogenides.[17] Lyotropic liquid crystal templating takes advantage of a self-assembled structure formed by a mixture of an amphiphile and water to control the structure of an inorganic phase; typically the inorganic phase grows in the hydrophilic domains of the liquid crystal, while the hydrophobic domains form the pores. Previously we combined lyotropic liquid crystal templating with colloidal templating in an approach we term "Double Direct Templaing" to form mesoporous hollow spheres (MHS).[18,19] In this approach, ZnS is heterogeneously nucleated onto a sacrificial core colloid within a lyotropic liquid crystal. After removal of the sacrificial core, the result is a ZnS MHS.

Here we demonstrate that a biomacromolecule, soybean peroxidase (SBP), can be encapsulated within a ZnS MHS and utilize the fixed mesopore size to entrap the SBP and regulate the transport of reactants through the shell. Small molecules (e.g., H_2O_2, NaN_3, and Amplex Ultra-Red) pass through the mesopores and interact with the SBP, while papain, a large protease, which can digest SBP, does not

* To whom correspondence should be addressed, pbraun@illinois.edu.
† Department of Materials Science and Engineering, University of Illinois at Urbana−Champaign.
‡ Frederick Seitz Materials Research Laboratory, University of Illinois at Urbana−Champaign.
§ Beckman Institute, University of Illinois at Urbana−Champaign.
⊥ Gerencia Química, Comisión Nacional de Energía Atómica.
DQIAyQF, FCEN, Universidad de Buenos Aires, Ciudad Universitaria.

10.1021/nl900264n CCC: $40.75
Published on Web 03/26/2009

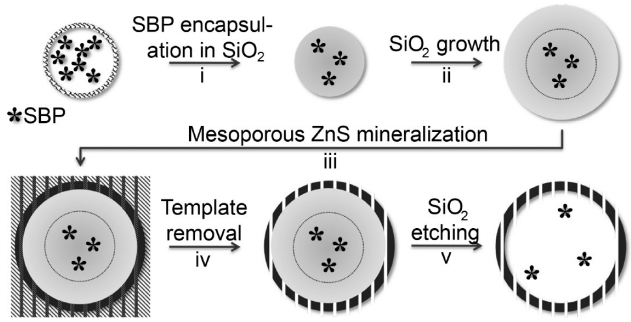

Figure 1. Procedure for encapsulation of soybean peroxidase (SBP) within a mesoporous ZnS hollow sphere: (i) utilizing a reverse emulsion, SBP is encapsulated within ca. 30 nm diameter SiO_2 colloids; (ii) the SiO_2 colloids are then grown to ca. 500 nm in diameter; (iii) mesoporous ZnS is mineralized onto the SiO_2 colloids utilizing a lyotropic liquid crystalline template; (iv) the template is then rinsed away; (v) the sacrificial SiO_2 template is etched, resulting in free SBP encapsulated within a ZnS MHS.

enter the MHS. SBP was specifically selected for encapsulation within MHS due to its size, thermal stability, activity over a wide pH range, and remarkable robustness.[20,21] SBP has molecular dimensions of 6.1 × 3.5 × 4.0 nm,[22] which are greater than the MHS mesopore diameter (ca. 3 nm),[17] and maintains similar dimensions when physisorbed onto a surface.[23] The MHS host has the unique advantage that the mesopores in the inorganic shell allow access to the encapsulated functional species by a size-selected range of reagents under a variety of environmental conditions. Additionally, the synthesis of the MHS is performed at room temperature with a mild chemical etching step, which is compatible with many organic, inorganic, and biological moieties. Moreover, the diameter of the sacrificial core can be used to vary the size of MHS.

Figure 1 outlines the procedure by which SBP was encapsulated within the ZnS MHS. First, a reverse emulsion was used to entrap the SBP within a sacrificial silica core. An aqueous solution of SBP (0.5 mL of 3 mg/mL) was added to a solution of 1.89 g of Triton X-100, 1.46 g of *n*-hexanol, and 5.84 g of cyclohexane.[24] To the reverse emulsion, 0.003 g of 3-triethoxysilylpropylamine (APTES), 0.094 g of tetraethyl orthosilicate, and 0.054 g of ammonium hydroxide (29%) was added to encapsulate SBP within SiO_2 colloids. The resulting colloids were thoroughly rinsed with acetone and ethanol via centrifugation and redispersion by sonication. The SBP loaded colloids were determined to be ca. 30 nm in diameter as measured by transmission electron microscopy (TEM). These colloids were further grown to ca. 500 nm by a seeded SiO_2 growth method based in a basic ethanolic hydrolysis.[25] Next, the colloids were functionalized with APTES.[26] The APTES functionalized SiO_2 (0.1% v/v) were then dispersed into an aqueous solution containing 0.01 M poly(acrylic acid) (MW = 2100 Da), which was bonded to the amine groups using 4-(4,6-dimethoxy[1.3.5]triazin-2-yl)-4-methylmorpholinium chloride hydrate.[27] The core colloids were then rinsed to remove excess poly(acrylic acid) and dispersed (0.02% v/v) in an aqueous solution containing 0.1 M zinc acetate and 0.1 M thioacetamide. The aqueous solution was then mixed with an equal weight of oligo(ethylene oxide) oleyl ether (Brij 97) to form the hexagonal lyotropic liquid crystalline template. Upon aging, a mesoporous ZnS shell heterogeneously mineralized onto the surface of the SiO_2 colloids.[18,19] Finally, the cores were etched with 5% hydrofluoric acid (HF) in ethanol, resulting in free SBP encapsulated within ZnS MHS. The MHS were then thoroughly rinsed with ethanol and redispersed in a PBS buffer (pH 7.4, 50 mM). TEM images of a ZnS MHS containing SBP after core etching at both low and high magnification, where the mesopore structure is evident, are shown in Figure 2. The high magnification image was taken from a particle with a thin, incomplete shell, where the mesopore structure is easy to observe. A more detailed analysis of the MHS mesostructure can be found in ref 19.

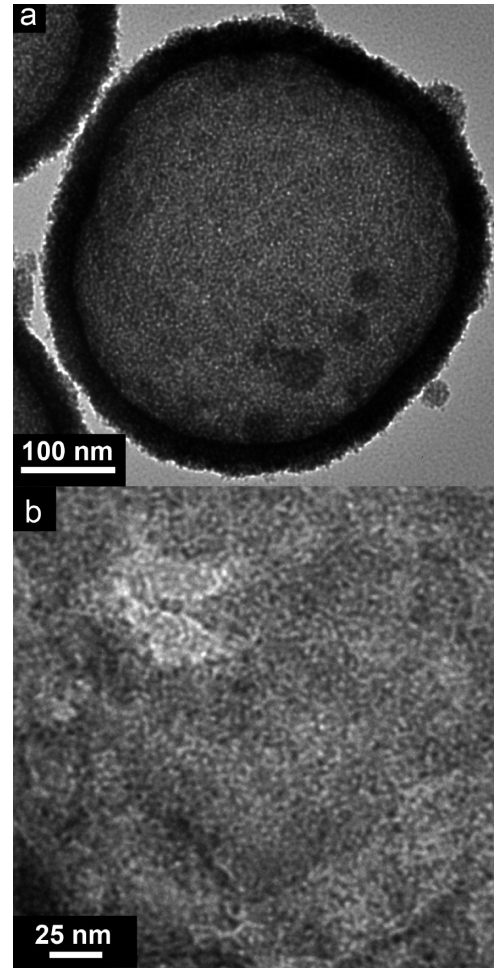

Figure 2. TEM images showing (a) a complete ZnS MHS containing SBP at low magnification and (b) a thin ZnS MHS at higher magnification where the mesopores are more evident.

The encapsulation efficiency of the reverse emulsion was determined by UV−visible spectroscopy by comparing the absorption of as-encapsulated SBP in SiO_2 with control samples of known SBP concentration, Figure 3. The scattering from the SiO_2 colloids was subtracted by matching the long wavelength absorbance of the SBP-containing sample with a control sample containing SiO_2 colloids. From the scatter-subtracted absorption of the SBP at 404 nm, an encapsulation efficiency of 10% was determined, which after

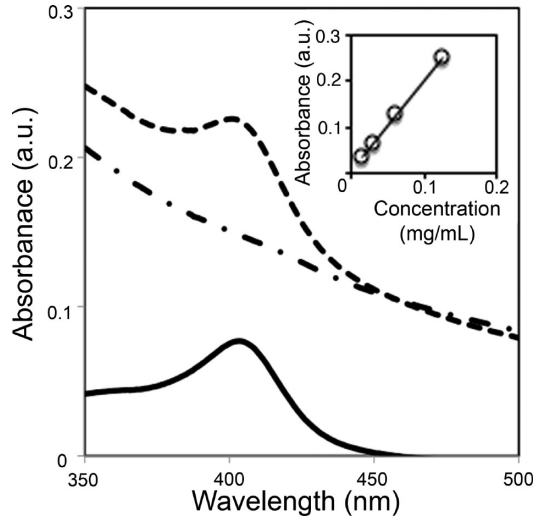

Figure 3. Absorbance vs wavelength for encapsulated SBP in SiO_2 (– – –). The SBP absorption (—) was calculated from the difference between as-encapsulated SBP in SiO_2 (– – –) and the scatter from a suspension of SiO_2 colloids (– • –). Inset: plot of the absorbance of known concentrations of SBP at a wavelength of 404 nm.

SiO_2 core etching corresponds to approximately eight enzyme molecules per MHS.

To verify the presence and catalytic activity of the MHS encapsulated SBP, a fluorogenic substrate, *N*-acetyl-3,7-dihydroxyphenoxazine (Amplex Ultra-Red), was utilized. Amplex Ultra-Red exhibits high reaction specificity with hydrogen peroxide in the presence of a peroxidase to form the fluorescent dye resorufin.[28,29] The activity of SBP after exposure to 5% HF in ethanol was verified by mixing the SBP powder with the ethanolic HF solution followed by dialysis against PBS to remove ethanol and HF. After this treatment, UV−visible spectroscopy confirmed SBP still catalyzed the formation of resorufin from Amplex Ultra-Red in the presence of hydrogen peroxide. Hydrogen peroxide, Amplex Ultra-Red, and resorufin are all smaller than the 3 nm diameter mesopores and thus are expected to pass rapidly through the MHS shell. A schematic of the peroxidase-catalyzed oxidation of Amplex Ultra-Red to resorufin is shown in Figure 4a(i). A fluorescence microscope was utilized to view the resorufin formed by the SBP catalyzed oxidation of Amplex Ultra-Red by exciting at wavelengths between 540 and 580 nm and collecting emitted fluorescence at wavelengths between 590 and 650 nm. ZnS MHS containing SBP were deposited onto glass coverslips covered with HybriWells (Grace Bio-Laboratories), and then the reagent solution (0.5 μM Amplex Ultra-Red and 0.018% by volume hydrogen peroxide in PBS) was injected into the sample well. Individual MHS were then observed to fluoresce (Figures 4b,c and 5). In the absence of SBP, fluorescent ZnS MHS were not observed, which is strong evidence both that active SBP is encapsulated and that ZnS does not catalyze the conversion of Amplex Ultra-Red to the dye resorufin.

The observed fluorescence emanating from the SBP-containing colloids is due to the production of resorufin in the core of the MHS (Figure 4a(i)). Upon elution of the

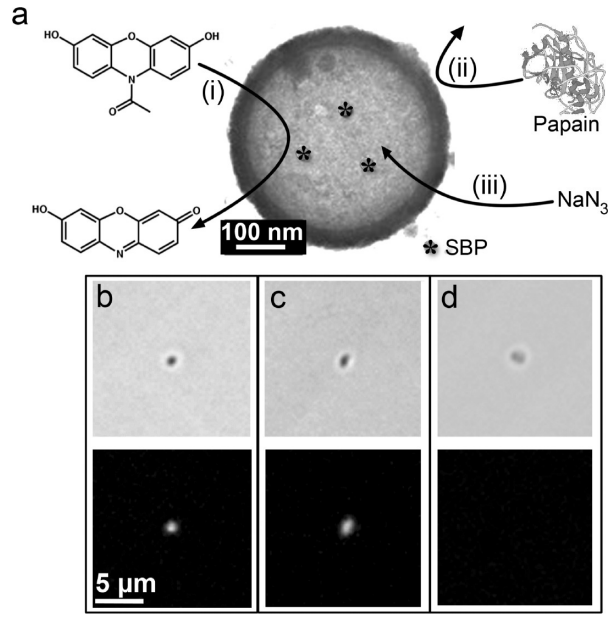

Figure 4. (a) Schematic representation of the interaction between different molecular species and the mesoporous ZnS shell: (i) the fluorogen, Amplex Ultra-Red, and H_2O_2 (not shown) enter the MHS and undergo a SBP-catalyzed reaction to form the dye resorufin; (ii) papain, a protease, was blocked from entering the MHS due to steric exclusion; (iii) NaN_3 readily entered the MHS to irreversibly inhibit SBP. Transmitted (top) and fluorescence (bottom) images of ZnS MHS containing SBP exposed to (b) Amplex Ultra-Red and H_2O_2, (c) Amplex Ultra-Red and H_2O_2 after exposure to papain, and (d) Amplex Ultra-Red and H_2O_2 after exposure to sodium azide. (All optical images are the same scale.)

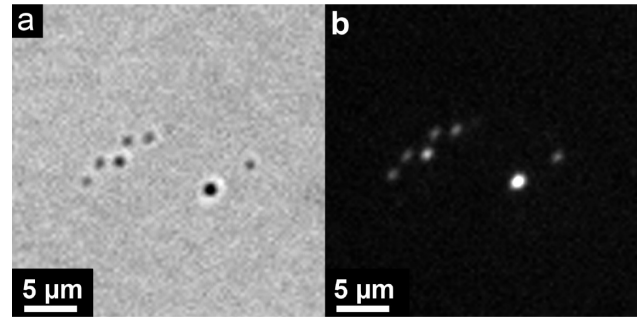

Figure 5. Transmitted (a) and fluorescence (b) light microscope images of ZnS MHS containing SBP in the presence of the fluorogen Amplex Ultra-Red and H_2O_2.

reagents with buffer solution, the MHS were observed to remain fluorescent, which implies adsorption of resorufin onto the ZnS shells. To verify that the observed fluorescence is due only to the SBP catalyzed oxidation of Amplex Ultra-Red, and not some other reaction, the fluorescence signal was observed as each component of the reagent solution (PBS, H_2O_2 in PBS, and Amplex Ultra-Red in PBS) was added individually to separate batches of the MHS containing SBP. Each sample was then subsequently eluted with the complete reagent solution. Fluorescence images were collected at 2 s intervals over 40 s after the addition of the individual components and for 40 s after elution with the complete reagent solution; plotted in Figure 6 are the fluorescence intensities of an individual MHS containing SBP

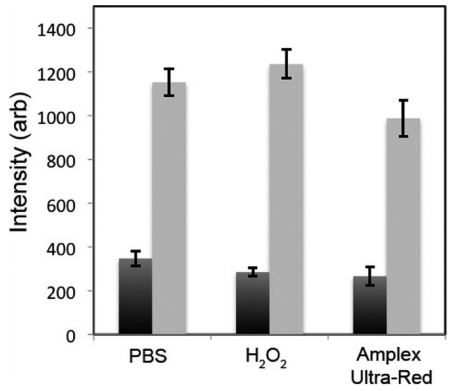

Figure 6. Plot of the average fluorescence intensities after exposure of MHS containing SBP to various reagent solutions. Initially, PBS, PBS containing H_2O_2, or PBS containing Amplex Ultra-Red was added to MHS containing SBP (black bars). The system was then eluted with the complete solution containing Ampex Ultra-Red and H_2O_2 in the PBS buffer (gray bars). The error bars indicate one standard deviation from the average fluorescence intensity over 40 s.

during each experiment. The error bars correspond to one standard deviation of the fluorescence intensity over 40 s for both the individual component and complete reagent solutions.

To demonstrate the size selectivity of the mesopores, papain, a cysteine protease, isolated from *papaya latex*, was mixed with the ZnS MHS containing SBP, Figure 4a(ii). Papain was chosen because it is larger than the mesopores,[30,31] and it has high, nonspecific activity[32] and well-understood activation/inhibition behavior.[30,31,33] This protease has molecular dimensions of ca. $5.0 \times 3.7 \times 3.7$ nm[31] and thus cannot fit through the 3 nm mesopores in the MHS. The protease was activated with dithiothreitol[33,34] and incubated with both the MHS containing SBP and free SBP in solution. The MHS were then thoroughly rinsed with the buffer solution to remove the protease and any digested SBP. Upon exposure to the Amplex Ultra-Red and H_2O_2 reagent solution, the MHS were observed to fluoresce (Figure 4c), indicating that the MHS protected the SBP by sterically excluding papain, while the protease digested any free SBP. To conclusively demonstrate that small molecules can permeate through the MHS shell wall, sodium azide (NaN_3), a known irreversible inhibitor for heme group containing enzymes, such as SBP, was also incubated with the MHS containing SBP (Figure 4a(iii)). Following incubation with NaN_3, the MHS were thoroughly rinsed with the buffer solution to remove excess NaN_3; upon introduction of the reagent solution, no fluorescence was observed in the sample (Figure 4d).

In summary, we described a general strategy for the encapsulation of an active biomolecular species within the central cavity of ZnS MHS. Both the activity of the encapsulated SBP and the size-selective transport through the wall of the MHS were verified through the use of a common fluorogen, hydrogen peroxide, and sodium azide. Additionally, the protection of the SBP was shown through size-selected blocking of papain. The mesoporous hollow sphere system introduces size selectivity to catalyzed chemical reactions; future work may include variations in pore sizes and pore wall chemical functionalization.

Acknowledgment. This work was supported primarily by the Nanoscale Science and Engineering Initiative of the National Science Foundation under NSF Award Number DMR-0642573. Dr. A. Wolosiuk is a permanent research fellow and member of Centro Interdisciplinario de Nanociencia y Nanotechnologia (CONICET) Argentina. This work was carried out in part in the Beckman Institute Microscopy Suite and in the Center for Microanalysis of Materials at the University of Illinois, which is partially supported by the U.S. Department of Energy under Grants DE-FG02-07ER46453 and DE-FG02-07ER46471. Enzyme graphics were adapted from the Protein Data Bank.

References

(1) Speir, J. A.; Munshi, S.; Wang, G. J.; Baker, T. S.; Johnson, J. E. *Structure* **1995**, *3* (1), 63–78.
(2) Douglas, T.; Strable, E.; Willits, D.; Aitouchen, A.; Libera, M.; Young, M. *Adv. Mater.* **2002**, *14* (6), 415.
(3) Douglas, T.; Young, M. *Nature (London)* **1998**, *393* (6681), 152–155.
(4) Donath, E.; Sukhorukov, G. B.; Caruso, F.; Davis, S. A.; Mohwald, H. *Angew. Chem., Int. Ed.* **1998**, *37* (16), 2202–2205.
(5) Lu, Y.; McLellan, J.; Xia, Y. N. *Langmuir* **2004**, *20* (8), 3464–3470.
(6) Xia, Y. D.; Mokaya, R. *J. Mater. Chem.* **2005**, *15* (30), 3126–3131.
(7) Caruso, F.; Caruso, R. A.; Mohwald, H. *Science* **1998**, *282* (5391), 1111–1114.
(8) Morishita, M.; Lowman, A. M.; Takayama, K.; Nagai, T.; Peppas, N. A. *J. Controlled Release* **2002**, *81* (1−2), 25–32.
(9) Mauser, T.; Dejugnat, C.; Sukhorukov, G. B. *J. Phys. Chem. B* **2006**, *110* (41), 20246–20253.
(10) Quinn, J. F.; Caruso, F. *Langmuir* **2004**, *20* (1), 20–22.
(11) Wang, Y. J.; Yu, A. M.; Caruso, F. *Angew. Chem., Int. Ed.* **2005**, *44* (19), 2888–2892.
(12) Mal, N. K.; Fujiwara, M.; Tanaka, Y. *Nature (London)* **2003**, *421* (6921), 350–353.
(13) Schuth, F.; Schmidt, W. *Adv. Mater.* **2002**, *14* (9), 629–638.
(14) Hernandez, R.; Tseng, H. R.; Wong, J. W.; Stoddart, J. F.; Zink, J. I. *J. Am. Chem. Soc.* **2004**, *126* (11), 3370–3371.
(15) Kanatzidis, M. G. *Adv. Mater.* **2007**, *19* (9), 1165–1181.
(16) Kresge, C. T.; Leonowicz, M. E.; Roth, W. J.; Vartuli, J. C.; Beck, J. S. *Nature (London)* **1992**, *359* (6397), 710–712.
(17) Braun, P. V.; Osenar, P.; Stupp, S. I. *Nature (London)* **1996**, *380* (6572), 325–328.
(18) Wolosiuk, A.; Armagan, O.; Braun, P. V. *J. Am. Chem. Soc.* **2005**, *127* (47), 16356–16357.
(19) Son, D.; Wolosiuk, A.; Braun, P. V. *Chem. Mater.* **2009**, *21*, 628–634.
(20) Blinkovsky, A. M.; Mceldoon, J. P.; Arnold, J. M.; Dordick, J. S. *Appl. Biochem. Biotechnol.* **1994**, *49* (2), 153–164.
(21) McEldoon, J. P.; Dordick, J. S. *Biotechnol. Prog.* **1996**, *12* (4), 555–558.
(22) Henriksen, A.; Mirza, O.; Indiani, C.; Teilum, K.; Smulevich, G.; Welinder, K. G.; Gajhede, M. *Protein Sci.* **2001**, *10* (1), 108–115.
(23) Karajanagi, S. S.; Vertegel, A. A.; Kane, R. S.; Dordick, J. S. *Langmuir* **2004**, *20* (26), 11594–11599.
(24) Jain, T. K.; Roy, I.; De, T. K.; Maitra, A. *J. Am. Chem. Soc.* **1998**, *120* (43), 11092–11095.
(25) Bogush, G. H.; Tracy, M. A.; Zukoski, C. F. *J. Non-Cryst. Solids* **1988**, *104* (1), 95–106.
(26) Vanblaaderen, A.; Vrij, A. *J. Colloid Interface Sci.* **1993**, *156* (1), 1–18.
(27) Kunishima, M.; Kawachi, C.; Hioki, K.; Terao, R.; Tani, S. *Tetrahedron* **2001**, *57* (8), 1551–1558.
(28) Zhou, M. J.; Diwu, Z. J.; PanchukVoloshina, N.; Haugland, R. P. *Anal. Biochem.* **1997**, *253* (2), 162–168.

(29) Zhou, M. J.; PanchukVoloshina, N. *Anal. Biochem.* **1997**, *253* (2), 169–174.
(30) Lowe, G. *Philos. Trans. R. Soc. London. Ser. B* **1970**, *257* (813), 237–248.
(31) Drenth, J.; Jansonius, J. N.; Koekoek, R.; Sluyterman, L. A. A.; Wolthers, B. G. *Philos. Trans. R. Soc. London, Ser. B* **1970**, *257* (813), 231–236.
(32) Grzywnowicz, K.; Brzyska, M.; Lobarzewski, J.; Greppin, H. *J. Mol. Catal.* **1992**, *77* (3), 365–376.
(33) Klein, I. B.; Kirsch, J. F. *J. Biol. Chem.* **1969**, *244* (21), 5928–5935.
(34) Grzywnowicz, K.; Brzyska, M.; Lobarzewski, J.; Greppin, H. *J. Mol. Catal.* **1992**, *77*, 365–376.

NL900264N